J Porous Mater (2015) 22:973–978
DOI 10.1007/s10934-015-9971-3

Preparation and characterization of high surface area ZrO_2 aerogel modified by SiO_2

Jing Ren[1] · Xiaobo Cai[1] · Hui Yang[1] · Xingzhong Guo[1]

Published online: 29 April 2015

Abstract Monolithic high surface area ZrO_2 aerogel modified by SiO_2 was successfully prepared by a sol–gel process followed by atmospheric pressure drying, using formamide as a drying control chemical additive and tetraethoxysilane solution for modification. The microstructure of the resultant core–shell ZrO_2/SiO_2 aerogel was characterized by scanning electron microscopy, X-ray photoelectron spectroscopy and transmission electron microscopy. Appropriate choice of formamide and tetraethoxysilane solution allowed the formation of the core–shell ZrO_2/SiO_2 aerogel with a BET surface area of 619 m^2/g, a pore size of 8.2 nm and a bulk density of 0.202 g/cm^3.

Keywords Aerogel · Zirconia · Atmospheric pressure drying · Sol–gel · Formamide

1 Introduction

Zirconia (ZrO_2) has been widely used as an advanced material in various areas such as electronics, optics, catalysis and high-temperature structural engineering due to its superior acidic and basic catalytic characters, redox properties, electrical properties and high thermal and chemical stability [1–7]. Aerogels are mesoporous solid materials composed of a three-dimensional network of nanoscale skeletons, and exhibit very high surface area and porosity, low density and a controllable structure. ZrO_2 aerogel has attracted much attention and has potential application such as catalyst supports and heat insulation materials because of their excellent properties combining zirconia with aerogel.

Many studies have been devoted to the synthesis of ZrO_2 aerogels. Several methods including precipitation, electrolysis and sol–gel process [8–12], and zirconium precursors, such as chloride, oxychloride, nitrate and alkoxides [4, 13, 14] have been used. The precipitation method is complicated and uncontrollable, and the electrolysis is high energy consumption. Moreover, the as-prepared aerogels are mainly powders or cracked fragments, greatly limiting the prolonged use. In contrast, the sol–gel method is an effective approach to prepare the aerogel products with high surface area and adjustable pore size distribution, as well as an excellent control of the properties. Recently, robust ZrO_2 aerogel with a monolithic shape has been prepared by modification of SiO_2 followed by supercritical drying. Immersing the wet gel in tetraethoxysilane solution leads to the deposition of a layer of SiO_2 on the surface of ZrO_2 gel particles and the formation of a core–shell nanostructure, and using supercritical drying enhances the network of ZrO_2 gel and prevents obvious shrinkage during drying [15, 16]. However, it is of high energy consumption and not a good choice for mass production.

In this study, we demonstrated an improved sol–gel route followed by atmospheric pressure drying to prepare high surface area ZrO_2 aerogel. In order to reduce the effect of capillary stress on gel skeletons during drying, formamide and tetraethoxysilane were used as drying control chemical additive and surface modifier, respectively. The effect of the amount of formamide and the concentration of tetraethoxysilane solution was investigated. The resultant core–shell ZrO_2/SiO_2 aerogels exhibit uniform porous structure, high surface area and low bulk density.

✉ Xingzhong Guo
msewj01@zju.edu.cn

[1] School of Materials Science and Engineering, Zhejiang University, Hangzhou 310027, People's Republic of China

2 Experimental section

2.1 Synthesis

Zirconyl nitrate ($ZrO(NO_3)_2{\cdot}5H_2O$) was utilized as a zirconium precursor. The mixture of distilled water and ethanol was used as the solvent, and PEG 400 was used as a dispersant. 1,2-Propylene oxide (PO) and formamide (FA) were added as gelation agent and drying control chemical additive, respectively. Alcoholic solution of tetraethoxysilane (TEOS) was used for modification. All reagents were used as received.

In a typical synthesis, certain amounts of $ZrO(NO_3)_2{\cdot}5H_2O$ and PEG 400 were dissolved in a mixture of distilled water and ethanol. Then, FA and PO were added in sequence under vigorous stirring. The concentration of the precursor solution was 0.3 mol/L. The samples with molar ratio of Zr(IV):PEG:PO:FA = 1:1:6:1.0, 1.5, 2.0, 2.5 were donated as FA10, FA15, FA20, FA25, respectively. After stirring at room temperature for 5 min, the containers together with the whole solution were placed at 60 °C for gelation. The wet gels were first solvent exchanged with ethanol (3 times × 12 h) and then immersed in 15 vol% TEOS solution for various time. The excessive TEOS in the gels was washed with ethanol (3 times × 12 h). The modified gels were dried in atmospheric pressure at 60 °C for several days and heat-treated at 1000 °C for 2 h with a heating rate of 5 °C/min.

2.2 Characterization

Morphologies and microstructure of zirconia aerogels were observed by scanning electron microscope (SEM: S4800, Hitachi, Japan) and transmission electron microscopy (TEM: Tecnai G2 F20, FEI, Holland). Bulk density was calculated from the weight/volume ratio of the aerogel samples. Meso- and micropores were characterized by N_2 adsorption–desorption isotherms (OMNISORP100CX, Beckman Coulter, USA) and the samples were first degassed at 100 °C. The surface area and pore size distribution were calculated using the Brunauer–Emmett–Teller (BET) and Barrett–Joyner–Halenda (BJH) method, respectively. The chemical states of oxygen atoms were recorded by X-ray photoelectron spectroscopy (XPS: Axis Ultra DLD, Kratos, UK), equipped with a hemispherical electron energy analyzer using a monochromatic Al Kα X-ray radiation. The crystalline phase was confirmed by powder X-ray diffraction (XRD: Empyrean 200895, PANalytical B.V., Holland).

3 Results and discussion

3.1 Effect of drying control chemical additive

In the present system, FA is added as a drying control chemical additive (DCCA). Figure 1 shows SEM images

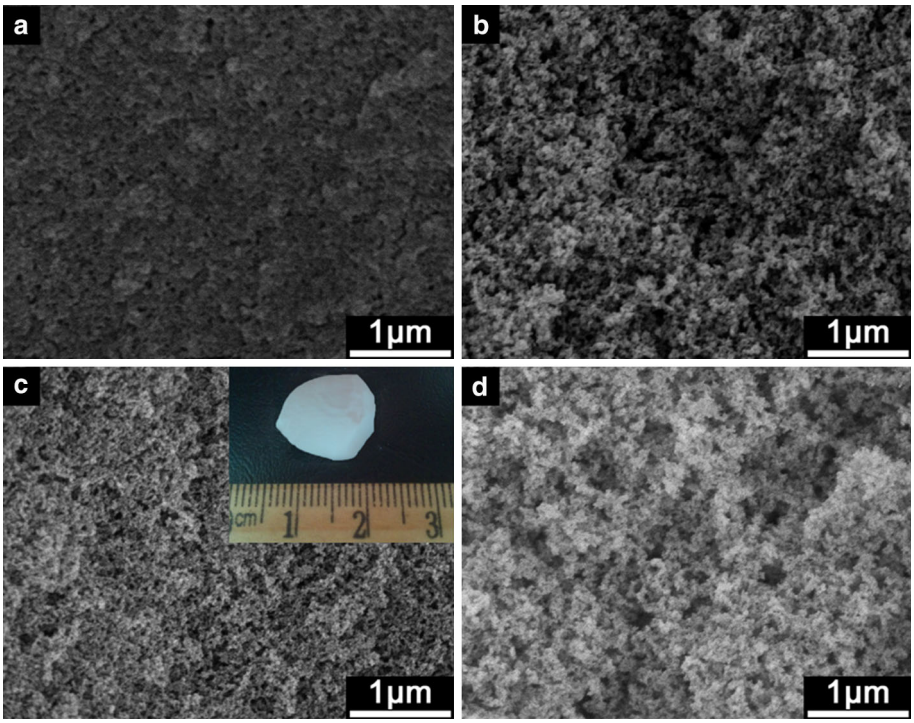

Fig. 1 SEM images of the core–shell ZrO_2/SiO_2 aerogels prepared with varied amounts of FA: **a** FA10, **b** FA15, **c** FA20, **d** FA25. *Inset* shows the appearance of FA20 core–shell ZrO_2/SiO_2 aerogel

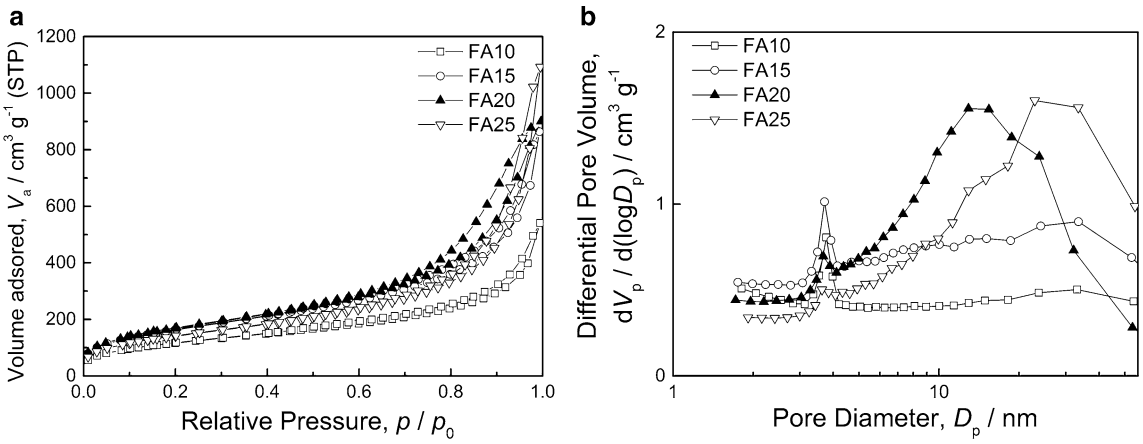

Fig. 2 **a** Nitrogen adsorption–desorption of the core–shell ZrO_2/SiO_2 aerogels prepared with varied amounts of FA and **b** the corresponding BJH pore size distribution curve

Table 1 Pore properties of the core–shell ZrO_2/SiO_2 aerogels prepared with varied amounts of FA

Samples	BET surface area (m^2/g)	Median pore size (nm)
FA10	430	7.4
FA15	602	8.1
FA20	619	8.2
FA25	520	12.4

of the core–shell ZrO_2/SiO_2 aerogels prepared with varied amounts of FA. All samples were treated with TEOS solutions for 48 h. When little FA is added, the gel exhibits obvious shrinkage after drying and few pores are observed (Fig. 1a). The morphology transforms to porous structure composed of loosely compacted particles with an increase in FA. Compared with sample FA15 and FA25, the pore size of FA20 is homogeneously distributed and the as-dried gel exhibits a monolithic shape.

Figure 2a shows nitrogen adsorption–desorption isotherms of the core–shell ZrO_2/SiO_2 aerogel prepared with varied amounts of FA. The corresponding BJH pore size distributions are shown in Fig. 2b. All samples exhibit isotherms of type IV according to the IUPAC classification, indicating the existence of mesopores. Revealed from BJH

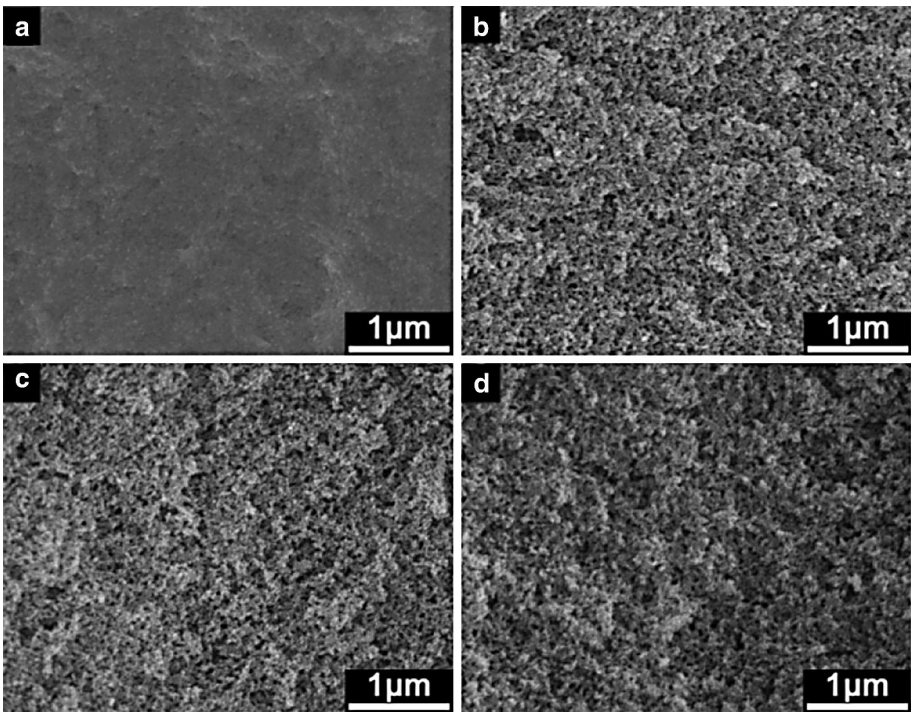

Fig. 3 SEM images of the core–shell ZrO_2/SiO_2 aerogels immersed in TEOS solution with varied time: **a** 0, **b** 24 h, **c** 48 h, **d** 72 h

data, FA15, FA20 and FA25 possess similarly pore size distribution and pores are distributed in the micro to mesopore region. The median pore size and BET surface area are summarized in Table 1. It shows that the BET surface area increases from 430 to 619 m^2/g and the median pore size increases from 7.4 to 12.4 nm with the addition of FA. It indicates that FA homogenizes the distribution of the pore size and reduces cracking caused by the pressure difference between adjacent holes. It enlarges the pore size of the gel network and reduces the capillary forces when drying. In addition, the bulk density of FA20 sample is calculated to be about 0.202 g/cm^3. The results of FA 20 sample are comparable with the ones by supercritical drying [16]. However, when too much FA is added, an obvious decrease in BET surface area is observed (520 m^2/g).

In addition, we can observe that the increase in the amount of FA also effectively shortens the gelation time from 37 (FA10) to 16 min (FA25). And a small increase will cause a significant change in the gelation time (from FA10 of 37 min to FA15 of 23 min) when only a little FA is added, indicating the sol–gel process is sensitive to FA in small amount range. FA can hydrolyze and form formic acid and ammonia under acidic solution:

$$HCONH_2 + H_2O \rightarrow HCONH_2 \cdot H_2O \rightarrow HCOOH + NH_3 \cdot H_2O$$

The reaction product $NH_3{\cdot}H_2O$ will increase the pH value, promoting the condensation like PO, so the gelation time decreases with an increased amount of FA [17, 18]. In fact, the reaction between formamide and water is suppressed at room temperature. After adding FA, the solution is transparent without significant change in pH value. Once placed at 60 °C, the hydrolysis reaction becomes faster, and ammonia is formed uniformly throughout the solution. In this system, the formation of uniform wet gels is a result of FA and PO [19]. The rest FA acts as DCCA to control the pore size and enhance the drying behavior of the gel network.

3.2 Effect of modification solution

Figure 3 shows SEM images the core–shell ZrO_2/SiO_2 aerogels immersed in TEOS solution with varied time. The wet gels are prepared from the starting compositions of FA20. When dried in atmospheric pressure directly, the gel becomes fragments after drying and almost no pores are

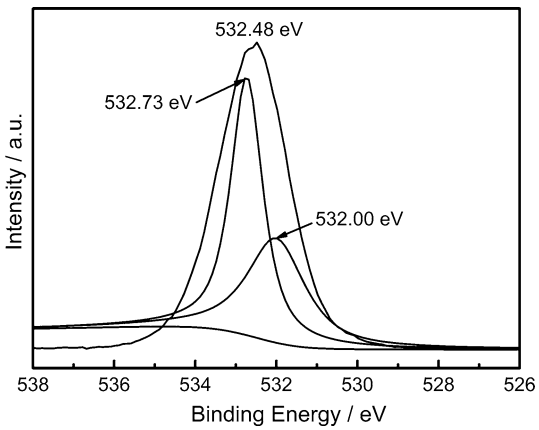

Fig. 4 O1s XPS spectra of the core–shell ZrO_2/SiO_2 aerogel

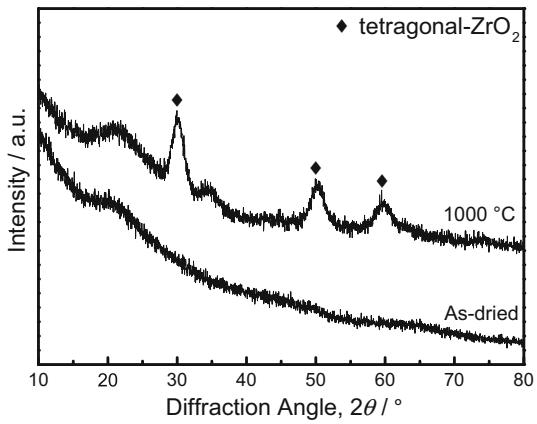

Fig. 6 XRD patterns of the core–shell ZrO_2/SiO_2 aerogels before and after heat-treatment

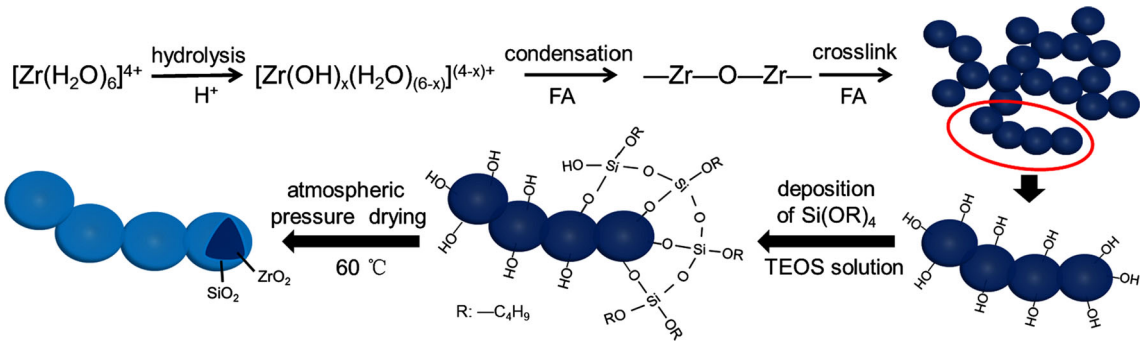

Fig. 5 Schematic representation of preparation of the core–shell ZrO_2/SiO_2 aerogel in this study

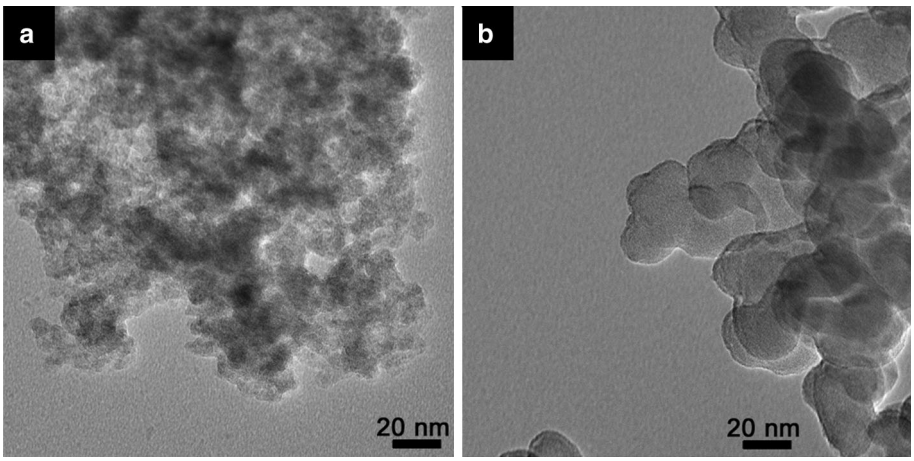

Fig. 7 TEM images of the core–shell ZrO_2/SiO_2 aerogels **a** as-dried and **b** heat-treated at 1000 °C

observed even appropriate amount of FA is added (Fig. 3a). After immersed in TEOS solution for 24 h, aerogel with uniform mesoporous structure is obtained (Fig. 3b). And it seems that the morphology does not change much with a longer immersion time.

For the core–shell ZrO_2/SiO_2 aerogel immersed in TEOS solution for 48 h, the corresponding XP levels of O1s exhibits at 532.48 eV, as shown in Fig. 4. The asymmetry of O1s peak indicates that the oxygen atoms in aerogel should be in more than one state. The peak-fits reveal a peak ascribed to the oxygen of Si–O at 532.73 eV and another one attributed to the oxygen of surface hydroxyls at 532.00 eV [20]. The result indicates that some SiO_2 generated from the hydrolysis of TEOS is deposited on the surface of ZrO_2 gel particles.

Figure 5 summarizes the sol–gel route and modification process for preparation of the core–shell ZrO_2/SiO_2 aerogel in this study. The core–shell ZrO_2 aerogel with high surface area can be obtained after atmospheric pressure drying mainly because of two factors. The utilization of FA as a gelation agent as well as a DCCA promotes the condensation process uniformly and modifies the polarity of gel skeletons [18]. The deposition of SiO_2 on the surface of primary particles forms a core–shell like structure, which can resist the capillary stress better [15].

3.3 Effect of heat-treatment

Figure 6 shows XRD patterns of the core–shell ZrO_2/SiO_2 aerogels before and after heat-treated at 1000 °C. The as-dried sample is amorphous. Diffraction peaks observed at about 30°, 50° and 60° on the heat-treated aerogel are attributed to tetragonal ZrO_2. The broad peaks mean crystalline microstructure with poor crystallinity, which suggests that the crystal growth is inhibited upon heat-treatment after modified by TEOS solution. It is also confirmed by TEM images, as shown in Fig. 7. The as-dried sample is made up of amorphous primary particles (Fig. 7a) and the heat-treated aerogel possesses nanocrystalline structure (Fig. 7b).

4 Conclusions

The core–shell ZrO_2/SiO_2 aerogel with high surface area is successfully prepared by a sol–gel process followed by atmospheric pressure drying. Formamide is added as a drying control chemical additive and tetraethoxysilane is used as a modifier. Under the molar ratio of Zr(IV):formamide = 1:2.0 and immersing the wet gel in tetraethoxysilane solution for 48 h, the resultant core–shell ZrO_2/SiO_2 aerogels possess a BET surface area of 619 m^2/g, a pore size of 8.2 nm and a bulk density of 0.202 g/cm^3, which are comparable with the ones by supercritical drying. The as-dried gel is amorphous and transforms to tetragonal ZrO_2 after heat-treated at 1000 °C, while the crystallization is inhibited.

Acknowledgments This work is supported by the National Natural Science Foundation of China (51372225).

Conflict of interest The authors declare that they have no conflict of interest.

References

1. T. Yamaguchi, Catal. Today **20**, 199 (1994)
2. P.D.L. Mercera, J.G. Van Ommen, E.B.M. Doesburg, A.J. Burggraaf, J.R.H. Ross, Appl. Catal. **57**, 127 (1990)
3. C. Morterra, G. Cerrato, S. DiCiero, M. Signoretto, F. Pinna, G. Strukul, J. Catal. **165**, 172 (1997)
4. M. Signoretto, L. Oliva, F. Pinna, G. Strukul, J. Non-Cryst. Solids **290**, 145 (2001)
5. S. Cimino, R. Pirone, L. Lisi, Appl. Catal. B **35**, 243 (2002)
6. A. Bahamonde, S. Campuzano, M. Yates, P. Salerno, S. Mendioroz, Appl. Catal. B **44**, 333 (2003)

7. K. Yamahara, T.Z. Sholklapper, C.P. Jacobson, S.J. Visco, L.C. De Jonghe, Solid State Ion. **176**, 1359 (2005)
8. A.F. Bedilo, K.J. Klabunde, Nanostruct. Mater. **8**, 119 (1997)
9. Q. Sun, Y.L. Zhang, J.F. Deng, S.Y. Chen, D. Wu, Appl. Catal. A **152**, 165 (1997)
10. Z.G. Wu, Y.X. Zhao, L.P. Xu, D.S. Liu, J. Non-Cryst. Solids **330**, 274 (2003)
11. N.C. Chervin, J.B. Clapsaddle, W.H. Chiu, A.E. Gash, J.H. Satcher, Chem. Mater. **17**, 3345 (2005)
12. R.H. Sui, A.S. Rizkalla, P.A. Charpentier, Langmuir **22**, 4390 (2006)
13. C. Stocker, A. Baiker, J. Non-Cryst. Solids **223**, 165 (1998)
14. H. Kalies, N. Pinto, G.M. Pajonk, D. Bianchi, Appl. Catal. A **202**, 197 (2000)
15. S.J. Shen, G. Wang, S.F. Jin, Q.Z. Huang, T.P. Ying, D.D. Li, X.F. Lai, T.T. Zhou, H. Zhang, Z.P. Lin, Chem. Mater. **26**, 5761 (2014)
16. Q.P. Wang, X.L. Li, W.P. Fen, H.M. Ji, X.H. Sun, R. Xiong, J. Porous Mater. **21**, 127 (2014)
17. N. Viart, J.L. Rehspringer, J. Non-Cryst. Solids **195**, 223 (1996)
18. A.V. Rao, H.M. Sakhare, A.K. Tamhankar, M.L. Shinde, D.B. Gadave, P.B. Wagh, Mater. Chem. Phys. **60**, 268 (1999)
19. X.Z. Guo, L.Q. Yan, H. Yang, J. Li, C.Y. Li, X.B. Cai, Acta Phys. Chim. Sin. **27**, 2478 (2011)
20. Z.Q. Zhao, X.L. Jiao, D.R. Chen, J. Mater. Chem. **19**, 3078 (2009)